

Occurrence of iron ores hosted in Los Tábanos Rhyodacite of San Juan del Cesar (La Guajira), Sierra Nevada of Santa Marta massif: petrologic significance

Manifestaciones de minerales de hierro alojados en la Riodacita de Los Tábanos de San Juan del Cesar (La Guajira), macizo de Sierra Nevada de Santa Marta: importancia petrológica

Carlos Alberto Ríos-Reyes ¹ Elías Ernesto Rojas-Martínez ² y Dino Carmelo Manco-Jaraba³

Fecha de Recepción: 11 de marzo de 2024

Fecha de Aceptación: 1 de marzo de 2025

Cómo citar: Ríos-Reyes., C.A.; Rojas-Martínez., E.E. y Manco-Jaraba., D. C. (2025). Occurrence of iron ores hosted in Los Tábanos Rhyodacite of San Juan del Cesar (La Guajira), Sierra Nevada of Santa Marta massif: petrologic significance, *Tecnura*, 29(83), 65-84. <https://doi.org/10.14483/22487638.21971>


Abstract

Context: Los Tábanos Rhyodacite, located in San Juan del Cesar (La Guajira) within the Sierra Nevada de Santa Marta Massif, exhibits outcrops affected by ongoing chemical weathering processes, primarily oxidation. This alteration results in the formation of iron minerals that provide relevant information on the petrological evolution of the rock.


Objective: To characterize the iron manifestations, evaluating their petrological significance and mineralogical phases.

Methodology: Representative samples were analyzed using complementary analytical techniques: stereomicroscopy, scanning electron microscopy (SEM), X-ray diffraction (XRD), wavelength-dispersive X-ray fluorescence (WD-XRF), attenuated total reflection infrared spectroscopy (ATR-IR), and Raman spectroscopy. These methods enabled the identification of mineral phases and the assessment of the mineralogical and microstructural complexity of the samples.

Results: Mineralogical analysis revealed the presence of magnetite, hematite, quartz, and actinolite. The data indicate that iron mineral occurrences develop primarily on recently fractured surfaces, where chemical weathering is

¹Geólogo. Universidad Industrial de Santander. Bucaramanga, Colombia. . Correo electrónico: carlosalbertoreyes@yahoo.es

²M. Sc. Geología Económica, Geólogo. Fundación Universitaria del Área Andina. Valledupar, Colombia. . Correo electrónico: eliaser@hotmail.com

³M. Sc. Gestión Ambiental y Energética en las Organizaciones, Ingeniero de Minas. Docente Ocasional Universidad de La Guajira. Riohacha. Colombia. . Correo electrónico: dinomancojaraba@gmail.com o dcmancoj@uniguajira.edu.co

active. Overall, the samples exhibit low mineralogical and microstructural complexity.

Conclusions: Los Tábanos Rhyodacite undergoes active oxidation process associated with the interaction of iron with oxygen and water. This process mainly produces magnetite and hematite, minerals that reflect the chemical conditions of the environment and the degree of alteration of the rock. The low mineralogical complexity observed suggests a relatively simple system of mineral transformation.

Keywords: Analytical techniques, Hematite, Iron ores; Magnetite; Los Tabanos Rhyodacite

Resumen

Contexto: La Riodacita Los Tábanos, localizada en San Juan del Cesar (La Guajira) dentro del Macizo de la Sierra Nevada de Santa Marta, presenta afloramientos con evidencias de procesos de meteorización química en curso, principalmente de oxidación. Esta alteración involucra la formación de minerales de hierro que aportan información relevante sobre la evolución petrológica de la roca.

Objetivo: Caracterizar las manifestaciones de hierro, evaluando su significado petrológico y fases mineralógicas.

Metodología: Se analizaron muestras representativas mediante técnicas analíticas complementarias: estereomicroscopía, microscopía electrónica de barrido (SEM), difracción de rayos X (XRD), fluorescencia de rayos X de longitud de onda dispersiva (WDXRF), espectroscopía infrarroja por reflexión total atenuada (ATR-IR) y espectroscopía Raman. Estas herramientas permitieron identificar fases minerales y evaluar la complejidad mineralógica y microestructural de las muestras.

Resultados: El análisis mineralógico reveló la presencia de magnetita, hematita, cuarzo y actinolita. Las observaciones indican que las manifestaciones de minerales de hierro se desarrollan principalmente en superficies recientemente fracturadas, donde la meteorización química está activa. En general, las muestras presentan baja complejidad mineralógica y microestructural.

Conclusiones: La Riodacita Los Tábanos experimenta un proceso de oxidación activo asociado a la interacción de hierro con oxígeno y agua. Este fenómeno genera principalmente magnetita y hematita, minerales que reflejan las condiciones químicas del ambiente y el grado de alteración de la roca. La baja complejidad mineralógica observada sugiere un sistema relativamente simple de transformación mineral.

Palabras clave: Hematita; Magnetita; Menas de hierro; Riodacita de Los Tábanos; Técnicas analíticas

Introducción

The Sierra Nevada de Santa Marta Massif (SNSM) (Figure 1) contains significant deposits of natural resources, including coal, marble, limestone, barite, and iron. Mining and quarrying activities in the region constitute an important source of raw materials and production, primarily through the extraction of these commodities. Among them, iron (Fe) represents a particularly promising target for exploration. Several projects have been initiated to evaluate the geological potential of iron ores, aiming to contribute to the socioeconomic development of the La Guajira department. These initiatives have included ore evaluation studies, extraction processes, and their potential applications.



Figura 1. *Left:* Satellite Google Earth image of the Sierra Nevada de Santa Marta Massif (SNSMM), showing the study area. *Right:* Satellite Google Earth image showing the distribution of sampling localities for iron ore occurrences hosted in Los Tábanos Rhyodacite of San Juan del Cesar (La Guajira)

Source: Author.

However, comprehensive research on the petrology and ore deposit geology of iron occurrences in this region remains limited. In particular, the genetic types of these deposits are still a matter of debate. In this context, mineralogical characterization using integrated analytical techniques is therefore crucial for understanding the genesis of these ores. Iron deposits can undergo multiple transformations under varying environmental conditions, resulting in a wide range of mineralogical and microstructural varieties (Cornell & Schwertmann, 2003). Due to the irregular distribution and uncommon concentration of these deposits, no universal classification exists for the geochemical anomalies they present. A useful approach to classify metallic deposits, based on geological environment, age, morphology, and mineralogy, distinguishes among iron formations, ironstones, and bog iron deposits (Stanton & Stanton, 1972).

The main iron-bearing minerals in these deposits include hematite (Fe_2O_3), magnetite (Fe_3O_4), limonite ($2\text{Fe}_2\text{O}_3 \cdot 3\text{H}_2\text{O}$), siderite (FeCO_3), and pyrite (FeS_2) (Ussher *et al.*, 2004). Geological evidence also indicates volcanic activity toward the southern sector of La Guajira, extending from the Triassic to the early Cretaceous. This magmatic event is represented by Los Tábanos Rhyodacite (Jt) (García-González *et al.*, 2009).

The purpose of this study is to present and discuss data concerning the iron ores hosted in Los Tábanos Rhyodacite of San Juan del Cesar (La Guajira). Specifically, the study aims to characterize the occurrence of these ores and assess their petrological significance. We suggest that this mineralization may serve as an important case study, providing new insights into volcanic-hosted Fe mineral occurrences in Colombia.

Regional Geology

The SNSM is located in the northwestern part of Colombia, covering an area of 13.700 km², with a maximum altitude of 5.900 m (Cardona *et al.*, 2010). The SNSM forms a triangular massif of several lithologies. Within the framework of the Colombian Andes, it has been the subject of numerous studies (Campbell, 1965; Cardona *et al.*, 2010a; Cardona *et al.*, 2010; Cordani *et al.*, 2005; Doolan & MacDonald, 1970; Herrera *et al.*, 2008; Irving, 1975; Kellogg, 1984; MacDonald *et al.*, 1971; Molina *et al.*, 2006; Montes *et al.*, 2010; Ordóñez *et al.*, 2002; Radelli, 1962; Restrepo-Pace *et al.*, 1997; C. Tschanz *et al.*, 1974; C. M. Tschanz *et al.*, 1969). Its geological evolution is the result of complex tectonic interactions among the Caribbean, South American, and Pacific plates during the Late Mesozoic to Cenozoic, which has triggered block rotation, basin formation and tectonic uplift in northern Colombia (Colletta *et al.*, 1997; Kellogg, 1984; Montes *et al.*, 2005, 2010). The massif is bounded by major faults and surrounded by Tertiary basins and the structural depression of the Cesar and Ranchería rivers. Its geological complexity reflects the effects of three major orogenic episodes and at least three periods of faulting. Two fault systems of particular importance in the tectonic evolution of northwestern South America affect the massif: the sinistral Santa Marta–Bucaramanga Fault and the dextral Oca Fault. Other major bounding structures include the he Oca fault (Irving, 1975), the Santa Marta-Bucaramanga fault (Campbell, 1965), the Cerrejón thrust sheet (Kellogg, 1984) and the Romeral suture (Montes *et al.*, 2010). The massif is mainly composed of crystalline rocks and comprises three geotectonic provinces (Sierra Nevada, Sevilla, and Santa Marta), having a defined outboard younging pattern from east to west. The Geotectonic Province of Sierra Nevada (GPSN) includes ca. 1.0-1.2 Ga high-grade metamorphic rocks (granulites, gneisses, and amphibolites) that were affected during the Grenvillian orogenic event (Herrera *et al.*, 2008; Restrepo-Pace *et al.*, 1997). Jurassic plutons and vulcanites intrude and cover these metamorphic rocks. Minor Carboniferous and Late Mesozoic sedimentary sequences rest in unconformity towards the southeast (Tschanz *et al.*, 1974; Tschanz *et al.*, 1969). The Geotectonic Province of Sevilla (GPSE) corresponds to a poly-metamorphic complex that includes Paleozoic gneisses and schists with Permian millonitized peraluminous granitoids (Cardona *et al.*, 2010b; Herrera *et al.*, 2008). The Geotectonic Province of Santa Marta (GPSM) comprises an inner sub-belt of Cretaceous imbricated metamorphic rocks (greenschists and amphibolites) and an outer sub-belt of Mesozoic amphibolites, greenschists and phyllites separated by the lower to middle Cenozoic Santa Marta Batholith (Doolan, 1970; Doolan & MacDonald, 1970).

Many tectonic models for the southern Caribbean postulate an accretion during the Late Cretaceous and/or Tertiary rocks of oceanic island arc of Mesozoic age. However, there are still numerous geological controversies yet to be resolved in relation to the studies performed by Radelli (1962) and Tschanz *et al.* (1969). In the study area, lithologies range from Precambrian

to Paleocene ages. These rocks include the oldest geological unit corresponding to Los Mangos Granulite (PEm); the volcanic rocks of the Golero Rhyolites (Jg), the volcano-sedimentary rocks of Los Tábanos Rhyodacite and Los Clavos Ignimbrite (Jt and Jlc); the plutonic igneous rocks of the Pueblo Bello and Patillal Batholith in its three phases, two granitic phases and one quartzmonzonitic phase (Jpbp); the sedimentary rocks represented by Cretaceous limestones and shales, the Guatapuri and Corual Formations (Kcsi, Tjg, PTc). Figure 2 shows a generalized geological map of the study area. Los Tábanos Rhyodacite are the rocks of interest in the present study. They include rhyolites of alkaline and calc-alkaline affinity with high potassium, as well as alkaline trachytes and some dacites.

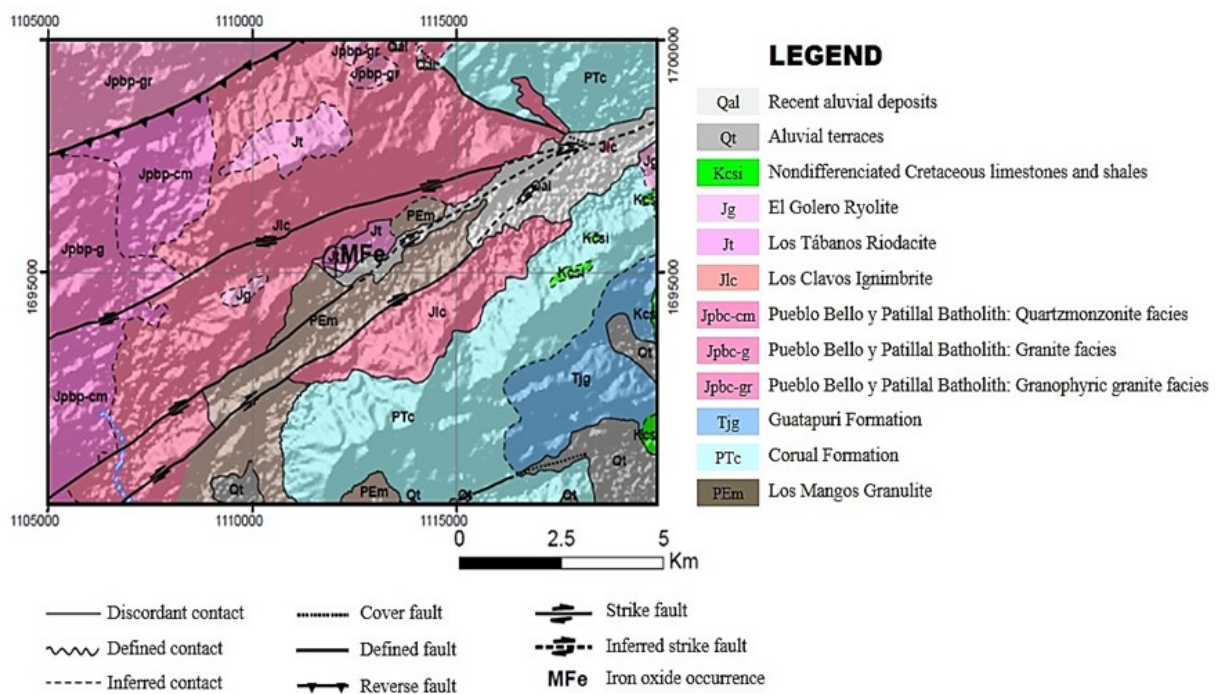


Figura 2. Generalized geological map of the study area

Source: Adapted and modified after (Colmenares *et al.*, 2007).

Methodology

A total of four samples were collected from several outcrops representing different lithological units (to be specified), which were subsequently prepared for laboratory analysis. A preliminary macroscopic description was followed by a visual inspection using a Zeiss Stemi DV4 binocular stereomicroscope, in order to identify the textural and structural features of the materials. For detailed characterization, the following analytical techniques were employed: X-ray powder diffraction (XRPD), field emission gun–environmental scanning electron microscopy

coupled with energy dispersive X-ray spectroscopy (FEG-ESEM/EDS), Fourier transform infrared spectroscopy with attenuated total reflection (FTIR-ATR), and X-ray fluorescence (XRF). The application of these methods has been previously described in detail in several works by Ríos and collaborators ([Bonilla-Jaimes *et al.*, 2016](#); [Castellanos-Alarcón *et al.*, 2016](#); [Lizcano-Cabeza *et al.*, 2015b, 2015a](#); [Ríos *et al.*, 2014](#)) and is summarized below.

The bulk mineralogical composition was determined by XRPD using a BRUKER D8 ADVANCE diffractometer operating in Da Vinci geometry. The instrument was equipped with a Cu-K α 1 X-ray tube ($\lambda = 1.5406 \text{ \AA}$), a one-dimensional LynxEye detector (aperture angle of 2.93°), a 0.6 mm divergent slit, two soller slits (primary and secondary, 2.5° each), and a nickel filter. Samples were ground in an agate mortar to a particle size of $< 50 \mu\text{m}$ and mounted on polymethylmethacrylate (PMMA) holders using the front-filling technique. Data were collected under the following conditions: 40 kV and 30 mA, over the 2θ range of $3.5\text{--}70^\circ$, with a step size of 0.01526° (2θ) and a counting time of 1 s/step. Phase identification was performed using the PDF-2 crystallographic database (ICDD) and the Search-Match program. Unit-cell parameters, atomic positions, peak broadening factors, and phase concentrations were refined by the Rietveld method using the MDI RIQAS software.

The microtextural features and chemical composition of the samples were examined using back-scattered electron (BSE) imaging and EDS analysis on a FEI QUANTA 650 FEG-ESEM. Analytical conditions included a magnification of 100–800 \times , working distance (WD) of 10.2–10.8 mm, accelerating voltage of 20 kV, BSED-ETD detector, combined BSE-SE mode, horizontal field width (HFW) ranging from 2.98 mm to 373 μm , and an EDAX APOLO X EDS detector with a resolution of 126.1 eV (Mn K α).

The structural characterization of functional groups was carried out by FTIR-ATR spectroscopy using a THERMO SCIENTIFIC IS50 spectrometer equipped with a diamond crystal, covering the spectral range of 400–4000 cm^{-1} .

Finally, the elemental composition of the samples was determined by wavelength-dispersive X-ray fluorescence (WDXRF) using a BRUKER S8 TIGER spectrometer (4 kW, Rh tube). The instrument was equipped with a flow sensor, scintillation crystals, interchangeable collimators, and specialized analyzers to minimize spectral overlap and improve detection sensitivity. For this analysis, samples were ground in an agate mortar, sieved to $< 38 \mu\text{m}$, and then calcined. The resulting powders were remilled and placed in plastic sample holders (34 mm diameter). Spectral data and elemental concentrations were processed using the QUANT-EXPRESS software, based on the fundamental parameter method, achieving detection limits in the mg/kg range for mineral samples.

Results

Fieldwork occurrence

The iron ores of interest in this study occur within Los Tábanos Rhyodacite (Jt), represented by a volcanic-sedimentary sequence of rocks with a porphyritic texture and acid-to-intermediate composition, including andesitic, dacitic and trachytic tuffs, as well as lytic tuffs with blocks of volcano-sedimentary fragments. These rocks can be classified as highly fractured rhyolites and trachytes (Colmenares *et al.*, 2007). Figure 3C illustrates locally flow structures, each of different color and texture, dominated by rocks of pink to very light purple color, with small phenocrysts of potassium feldspar). Figure 3A shows a pink to orange- pink color, with sporadic pink feldspar phenocrysts, as well as typical light pink, pink orange, very light purple or reddish gray aphanitic felsic rocks with several flow structures, often containing small feldspar phenocrysts. According to (Colmenares *et al.*, 2007), based on a K-Ar dating in a crystal of sanidine of an obsidian 142 ± 6 Ma assigned an Upper Jurassic age for Los Tábanos Rhyodacite. Figure 3 illustrates the occurrence of outcrops of Los Tábanos Rhyodacite hosting iron ores. Field observations of the outcrops reveal rocks ranging from fresh to a moderately weathered. These rocks present their joint sets and other randomly orientated joints, which display similar characteristics with little variations. The openings of these discontinuity structures generally are classified as moderately spaced. The changes in the joint sets properties induced by weathering in Los Tábanos Rhyodacite are mainly of mineralogical type, developing late-stage oxidation halos (~5 mm) slightly stained with magnetite and hematite, which progressively decrease inward fresh rock.

Petrography

The host rock (rhyodacite) exhibits a holocrystalline texture with an inequigranular distribution of grains, and color index of 35 %. It is composed of plagioclase 50 % quartz 25 %, and feldspar 25 %, with secondary minerals as hematite and magnetite (/25 %). Hand specimens of Los Tábanos Rhyodacite show a freshly broken surface characterized by differential chemical weathering—probably mostly oxidation— progressing inward (Figure 4). This case accurately illustrates chemical weathering by oxidation, a process in which water and oxygen infiltrate the rock, reacting with ferrous minerals and generating oxides that modify its internal structure, color, and resistance. At the macroscopic scale, the analyzed samples of iron ores reveal a massive appearance of a thin skin mainly composed of magnetite-hematite of brown reddish color. The oxidation crust around the outside of the rock displays an inner white layer where the rhyodacite's minerals are beginning to break down and an outer red layer where magnetite and hematite are formed.



Figura 3. Outcrops of iron ores-hosted in Los Tabanos Rhyodacite, San Juan del Cesar (La Guajira), SNSM

Source: Author.

Scanning electron microscopy

Figure 5 presents SEM photomicrographs of the analyzed iron ores. Energy dispersive X-ray spectrometry (EDS) on scanning electron microscopy offer advanced analysis options for quantitative mineralogy and ore characterization ([Salge *et al.*, 2001](#)). In this study, metal oxides were analyzed by measuring both the metal and oxygen peaks. However, distinguishing between hematite and magnetite requires careful evaluation of analytical consistency and precision. In addition, it is necessary to properly clean and polish samples and account for sample charging, sample homogeneity and other systematic sources of error ([Konopka, 2012](#)).

The EDS analyses proved the presence of iron oxide minerals. Figure 6 shows a typical EDS spectrum of the analyzed iron ores showed the presence of high concentration of Fe (64.35-70.80 wt %) and O (21.84-29.19 wt %). The peak of C is attributed to the carbon coating. The peaks of Si, Mg, Al, Ca and Mn (results not shown) represent the contribution of quartz and actinolite

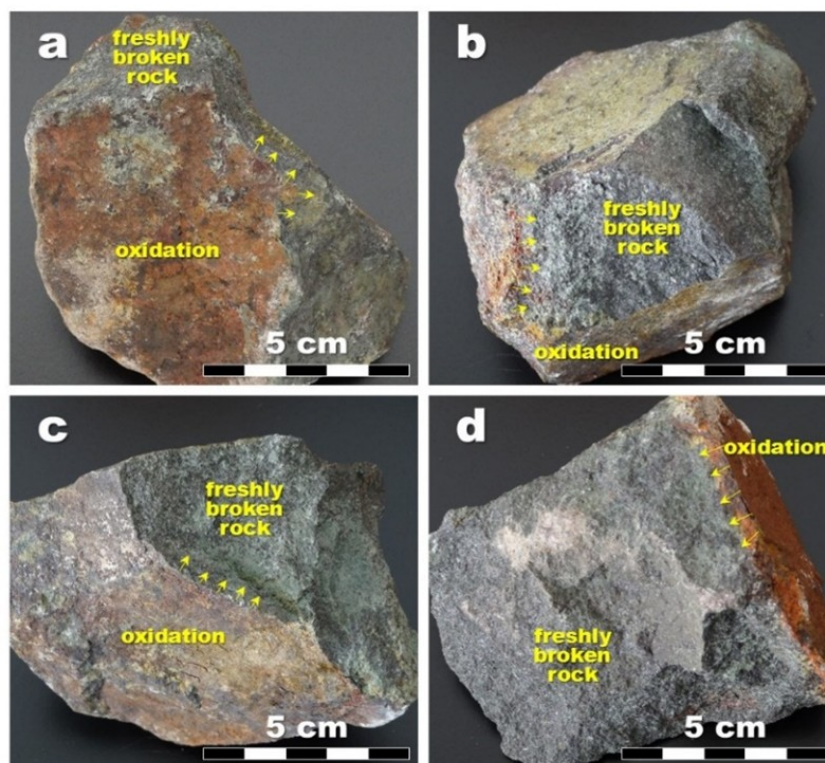


Figura 4. Photographs of hand specimens of Los Tábanos Rhyodacite of the San Juan del Cesar (La Guajira), SNSM, displaying oxidation

Source: Author.

of the rhyodacite hosting rock. According to [Paciornik and Gomes \(2009\)](#), the discrimination of hematite and magnetite in backscattered electron images requires an extreme contrast in the image, which precludes the segmentation of other phases. On the other hand, even automated SEM systems with X-ray energy dispersion microanalysis (EDS) cannot differentiate between hematite and magnetite. Thus, the quantitative microstructural characterization of iron ores remains a challenge.

X-RAY diffraction

The analyzed samples contain 18.9-21.2 % of magnetite, 21.6-24.2 % of hematite, 9.4-8.7 % of quartz and 6.4-8.6 % of actinolite as crystalline mineral phases, and 27.3-41.9 % of amorphous and other mineral phases. The X-ray diffraction pattern obtained by quantitative analysis is presented in Figure 7. The iron oxides (magnetite and hematite) have different crystal structures and, therefore, they have different patterns of X-ray diffraction. XRD pattern reveals that analyzed sample corresponds to a mixture of the two oxides.

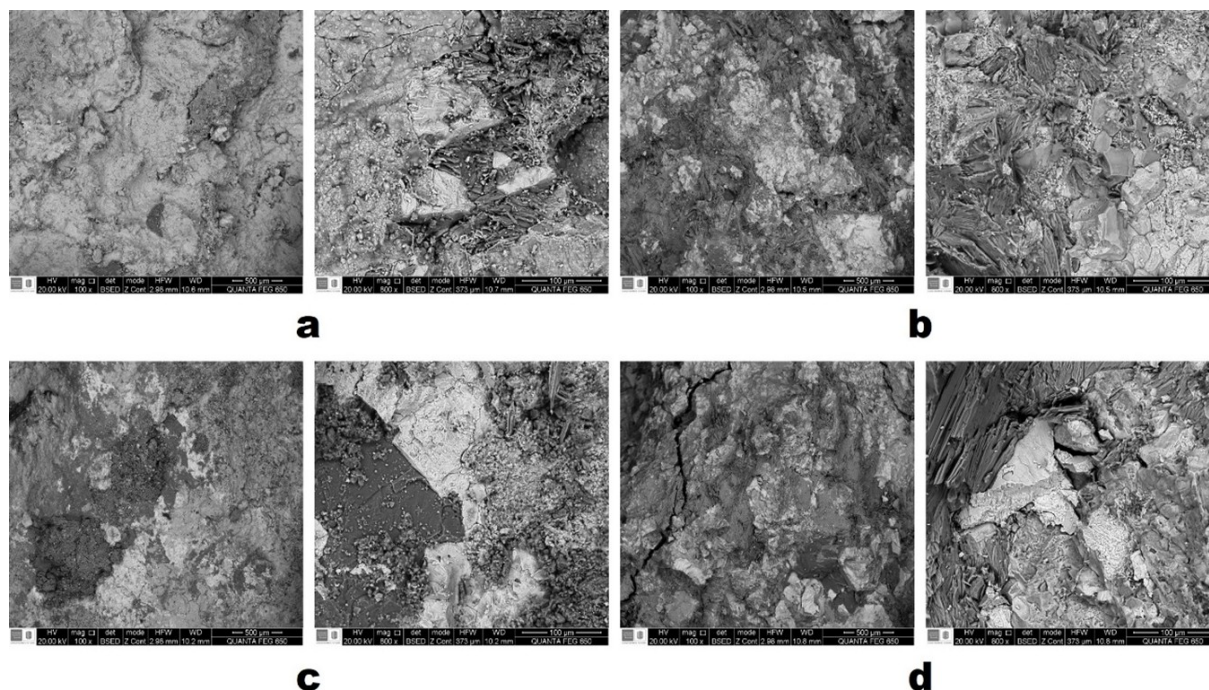


Figura 5. SEM photomicrographs of the analyzed iron ores

Source: Author.

Raman spectroscopy

Figure 8 illustrates the Raman spectra of the iron ores hosted in Los Tábanos Rhyodacite. The assignment of vibration band positions and the identification of the mineral phases were based on combined Raman data for the main vibration bands of iron oxides (*e.g.*, [De Faria *et al.*, 1997](#); [Shebanova & Lazor, 2003](#)), which for Fe_3O_4 are 193 (weak), 306 (weak), 538 (weak), 668 (strong); for $\alpha\text{-Fe}_2\text{O}_3$ are 225 (strong), 247 (weak), 299 (strong), 412 (strong), 497 (weak), 613 (medium); for $\gamma\text{-Fe}_2\text{O}_3$ are 350 (strong), 500 (strong), 700 (strong). The characteristic peak positions of magnetite (Fe_3O_4), hematite ($\alpha\text{-Fe}_2\text{O}_3$) and maghemite ($\gamma\text{-Fe}_2\text{O}_3$) were determined in the Raman region of interest in this investigation: $50\text{--}1500\text{ cm}^{-1}$. In the Raman spectra, the characteristic peaks of magnetite (Fe_3O_4) at 200, 463, 579, 661 and 669 cm^{-1} and hematite ($\alpha\text{-Fe}_2\text{O}_3$) at 222, 242, 288, 405, 496 and 1300 cm^{-1} and maghemite ($\gamma\text{-Fe}_2\text{O}_3$) at 391 cm^{-1} are observed.

Chemical analysis

Iron ores are disseminated Los Tábanos Rhyodacite. The concentration of Fe_2O_3 ranges from 64.21 to 78.35 % with sample YJ-1 and YJ-3 revealing the highest (78.35 %) and lowest (64.21 %) concentration of Fe_2O_3 . This variation can be attributed to the dissemination of the

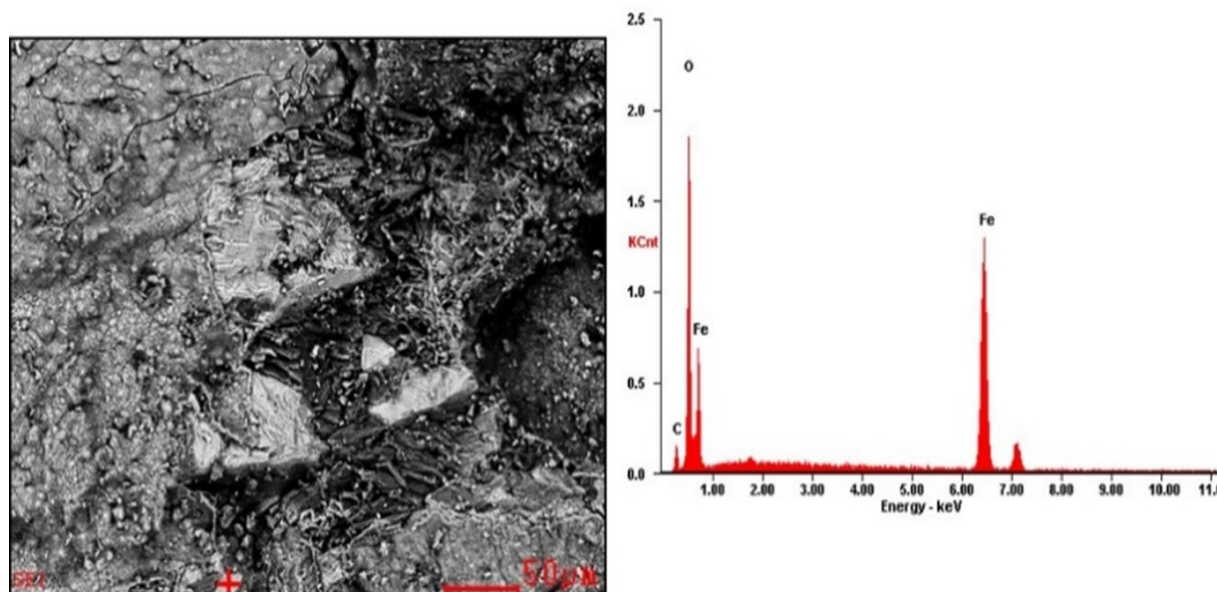


Figura 6. EDS spectrum of analyzed iron ores by EDS

Source: Author.

iron ores in the rock. Al_2O_3 show a very low concentration (0.56-0.72 %). The concentrations of CaO and MgO are 1.64-1.96 % and 2.17-2.54 %, respectively. K_2O and TiO_2 show a constant concentration (0.02 %). MnO concentration ranges from 0.28 to 0.33. The concentration of SiO_2 (15.40-30.17 %) can be mainly related to the presence of quartz in the host rock. The major oxide results generally reflect the mineralogical composition of the iron ores disseminated in the rhyodacite (Table 1).

Tabla 1. Major chemical composition of the analyzed samples of metal oxides (in %).

	YJ1	YJ2	YJ3	YJ5
SiO_2	15.40	27.16	30.17	24.94
Al_2O_3	0.72	0.65	0.56	0.66
CaO	1.96	1.64	1.69	1.70
MgO	2.32	2.17	2.32	2.54
K_2O	0.02	0.02	0.02	0.02
TiO_2	0.02	0.02	0.02	0.02
MnO	0.33	0.26	0.28	0.28
Fe_2O_3	78.35	67.20	64.21	69.07

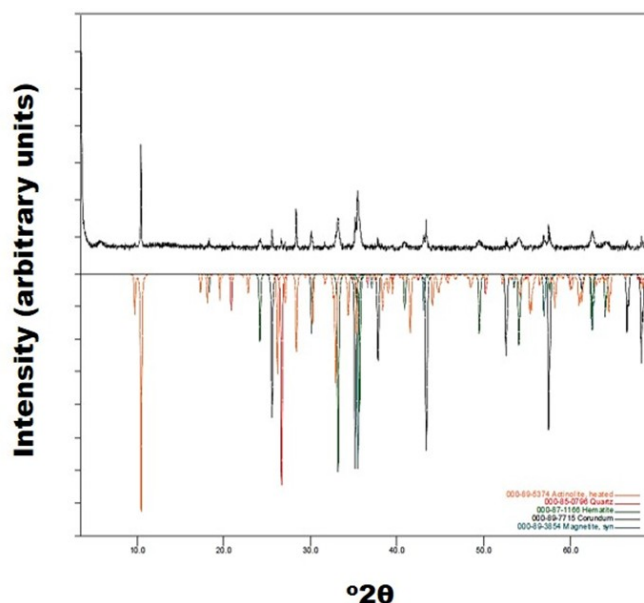


Figura 7. XRD pattern of the iron ores hosted in Los Tabanos Rhyodacite (qualitative analysis)

Source: Author.

Origin of the iron ores

Weathering is the physical disintegration and chemical decomposition of igneous rocks into soil, dissolved chemical components, and solid chemical residues (Formoso, 2006). These rocks are most stable under the pressure, temperature, and environmental conditions present during their crystallization. When exposed to near-surface conditions, however, they are no longer in equilibrium and become progressively affected by weathering.

Los Tábanos Rhyodacite's rocks crystallized under pressure and temperature conditions markedly different from those at the surface. Consequently, its primary minerals are unstable and undergo chemical reactions that alter their original composition (Figure 9). Physical weathering causes the disintegration of igneous rocks without chemical change. It can occur due to temperature, pressure, frost, etc. Los Tábanos Rhyodacite rocks were affected by physical weathering resulting in changing solid, large rock into smaller, movable unconsolidated debris, which was probably driven by changes in pressure and temperature conditions and organic activity. Chemical weathering is a gradual and ongoing process as the mineralogy of igneous rocks adjusts to the near surface environment, which occurs mainly at the surface of these rocks with the formation of secondary minerals develop from the original rock-forming minerals.

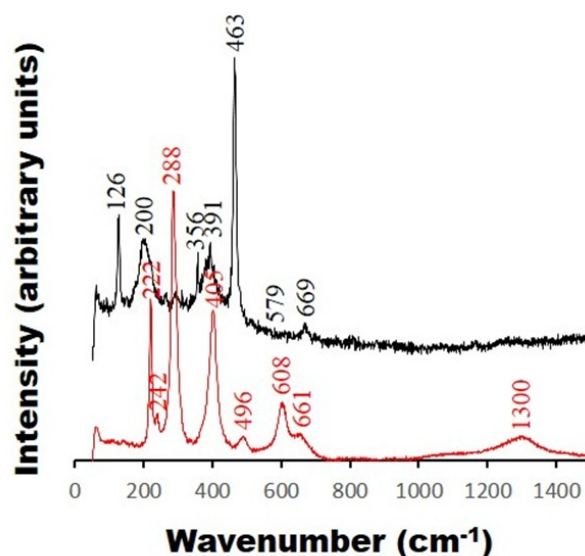


Figura 8. Raman spectra of mineral phases identified as magnetite (Fe_3O_4), hematite ($\alpha\text{-Fe}_2\text{O}_3$) and maghemite ($\gamma\text{-Fe}_2\text{O}_3$)

Source: Author.

Los Tábanos Rhyodacite's rocks were affected by oxidation, one of the more common and visible forms of chemical weathering. This reaction involves oxygen combining with minerals, particularly those containing iron to form iron oxide (rust). Therefore, the weathered region consists of rusty spots weaken these rocks and they break apart, which can be explained taking into account that iron oxide is much more fragile than iron, so. As a consequence of this process, the mineral compositions and the color of these rocks changed in the weathered region. Chemical weathering becomes more effective as the surface area of the rock increases ([Sharma, 2014](#)). In the case of rocks belonging to the Rhyodacite's Los Tábanos Unit, it is likely that the alterations observed are mainly due to chemical reactions occurring on their exposed surfaces. However, it should be noted that the smaller the particle size, the greater the surface-to-volume ratio, which increases the specific area available for chemical interaction. According to [Lapakko et al. \(2006\)](#), the kinetics of these reactions are usually directly proportional to the surface area of the mineral exposed to the reactive medium.

In this study, a clear oxidation process is recognized in Los Tábanos Rhyodacite, driven by the interaction of iron and oxygen in the presence of water and the main products of oxidation are magnetite and hematite. It strongly affected these rocks, which supposes the presence of abundant water. Oxygen molecules (O_2) collide with iron atoms of rock forming-minerals on

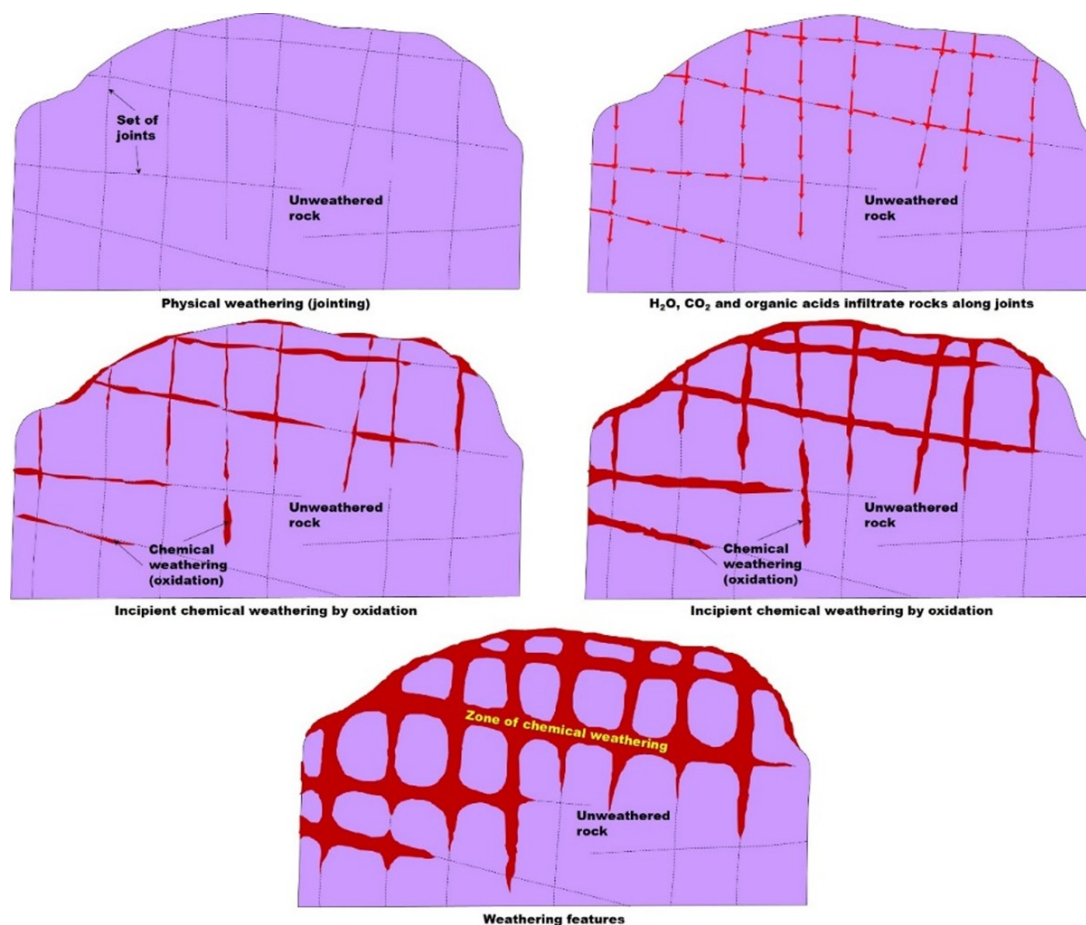


Figure 9. Diagram showing set of joints, promoting the chemical weathering

Source: Author.

the surface of the rock, which react to form iron oxide (rust) (Figure 10). Oxygen is a highly reactive gas that combines readily with other elements, such as iron. Rock-forming minerals of Los Tábanos Rhyodacite reacted directly with oxygen in the air to form iron oxides. However, the formation of rust after reaction of oxygen molecules and iron atoms was probably carried out in the presence of water, which is referred in this study as oxidation, a term for reactions in which iron atoms lose electrons and become more positively charged.

Evidently, Los Tábanos Rhyodacite's rocks contained iron-rich minerals that were broken down when exposed to the atmosphere, making them susceptible to chemical weathering. The main chemical reactions associated with chemical weathering are dissolution, hydrolysis, and oxidation (Ahluwalia, 2017). Oxidation occurred when oxygen reacted with iron-rich minerals to form iron oxide minerals. The absorption is usually from O_2 dissolved in soil water and that

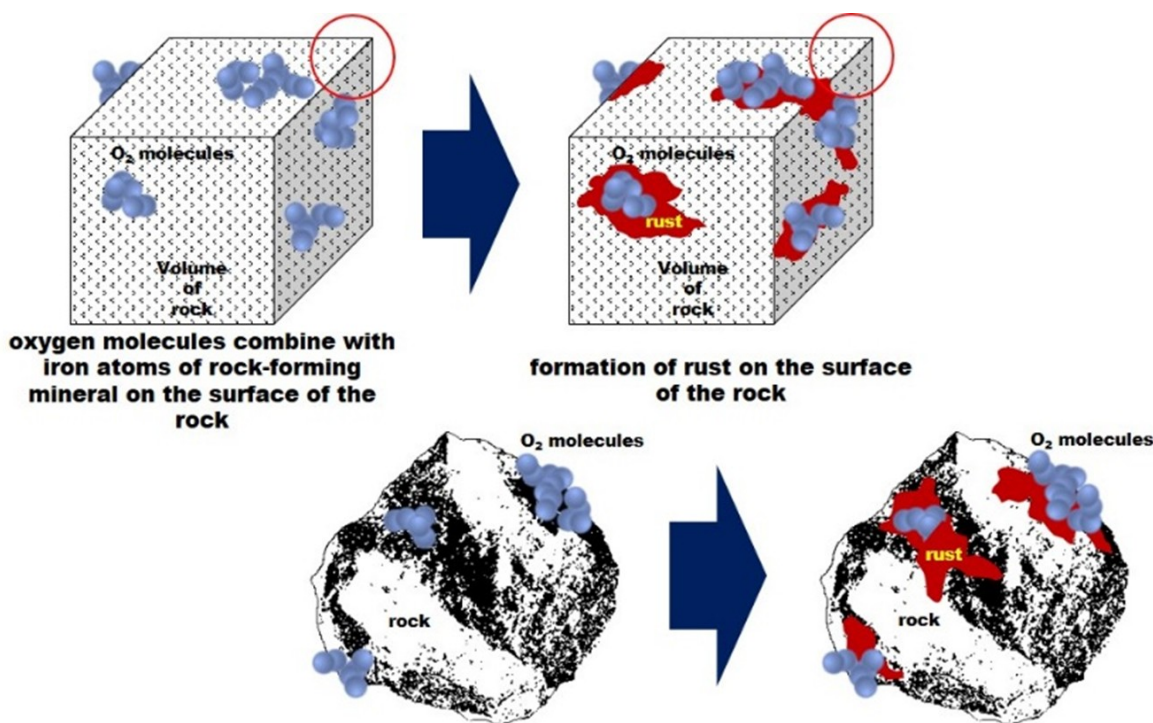
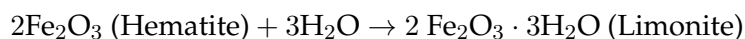
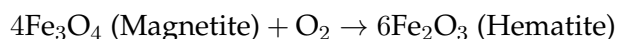
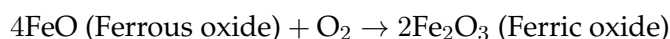


Figura 10. Diagram showing the process of oxidation

Source: Author.

present in the atmosphere and the oxidation is more effective in the presence of moisture and results in hydrated oxides (Rathinasamy & Saliha, 2017). According to these authors, during the oxidation processes, the following main chemical changes occur: (1) oxidation, solution and removal of the material, and (2) in situ transformation of rock-forming minerals into oxidized compounds.



As noted by Arikan and Aydin (2012), an increase in Fe₂O₃ content with increasing weathering indicates that oxidation plays a central role not only in the weathering of rocks of interest in the present study but also in the chemical transformation of iron minerals.

Rocks from Los Tábanos Rhyodacite are characterized by late-stage oxidation halos (~ 5 mm), which are common along joints. The exposure of these rocks to the weathering and its surface area affected its rate of weathering. The chemical weathering of these rocks occurs by the solution of Fe-rich mineral phases and tends to be concentrated at the rock surface or along joints, and a key element is the presence of water. Dissolution obviously occur, also acts as a medium for transporting acids, etc. Rainwater is acidic by nature due to atmospheric CO₂, which reacts with water to form carbonic acid. However, a hydration process appear to have had little effect on the rock-forming minerals, as indicated by the absence of limonite; thus, there is no evidence of the conversion of iron oxides to iron hydroxides. The occurrence of iron oxides magnetite (Fe₃O₄) and hematite (Fe₂O₃) hosted in Los Tábanos Rhyodacite of San Juan del Cesar (La Guajira), SNSM, consist of more than 60 % magnetite-hematite but those present a structural pattern similar to that of the lava mafic flows. Iron minerals, such as those reported in this study, can represent a rare case of an effusive Fe oxide liquid ([Dare et al., 2015](#)), however, fieldwork and petrographic evidences suggest that these probably are the result of the replacement of rhyodacite flows, with the development of magnetite-hematite pseudomorphs after rock-forming minerals.

Conclusion

The occurrence of iron minerals hosted in Los Tábanos Rhyodacite of San Juan del Cesar (La Guajira), Sierra Nevada of Santa Marta Massif, reveals that iron minerals occur in a freshly broken surface as a result of a chemical weathering process—probably mostly oxidation. The main products of oxidation are magnetite and hematite (α -Fe₂O₃) with traces of maghemite (γ -Fe₂O₃). The combination of analytical techniques, such as scanning electron microscopy, X-ray diffraction, and Raman spectroscopy is very useful for rapid, semiquantitative characterization of iron ore mineralogy. These techniques were well concurring with each other. Los Tábanos Rhyodacite's rocks were affected by the oxidation as a result of the reaction of oxygen with minerals, particularly those containing iron to form iron oxide (rust).

Acknowledgements

We gratefully acknowledge the University Foundation of the Andean Area, sectional Valledupar, for the support offered for the development of fieldwork, as well as the participation of students of Geological Engineering. The authors are indebted to the laboratories of Microscopy, X-Ray and Spectroscopy of the Universidad Industrial de Santander at the Guatiguará Technological Park and their responsible professional staff for technical support. This work benefited from constructive comments and suggestions provided by the Journal of Geoscience and Environment Protection editor and anonymous reviewers.

References

- Ahluwalia, V. K. (2017). *Advanced Environmental Chemistry*. The Energy and Resources Institute (TERI).
- Arikan, F., & Aydin, N. (2012). Influence of weathering on the engineering properties of dacites in Northeastern Turkey. *International Scholarly Research Notices*, 1–15.
- Bonilla-Jaimes, J., Henao-Martínez, J., Mendoza-Luna, C., Castellanos-Alarcón, O., & Ríos-Reyes, C. (2016). Non-destructive in situ analysis of garnet by combining scanning electron microscopy and X-ray diffraction techniques. *Dyna*, 83(195), 84–92. <https://doi.org/10.15446/dyna.v83n195.46360>
- Campbell, C. J. (1965). *The Santa Marta wrench fault of Colombia and its regional setting: Transactions of the Caribbean Geology Conference 4*, 247–261.
- Cardona, A., Valencia, V., Bustamante, C., García-Casco, A., Ojeda, G., Ruiz, J., Saldarriaga, M., & Weber, M. (2010a). Tectonomagmatic setting and provenance of the Santa Marta Schists, northern Colombia: Insights on the growth and approach of Cretaceous Caribbean oceanic terranes to the South American continent. *Journal of South American Earth Sciences*, 29(4), 784–804.
- Cardona, A., Valencia, V., Bustamante, C., García-Casco, A., Ojeda, G., Ruiz, J., Saldarriaga, M., & Weber, M. (2010b). Tectonomagmatic setting and provenance of the Santa Marta Schists, northern Colombia: Insights on the growth and approach of Cretaceous Caribbean oceanic terranes to the South American continent. *Journal of South American Earth Sciences*, 29(4), 784–804. <https://doi.org/10.1016/j.jsames.2009.08.012>
- Cardona, A., Valencia, V., Garzón, A., Montes, C., Ojeda, G., Ruiz, J., & Weber, M. (2010). Permian to Triassic I to S-type magmatic switch in the northeast Sierra Nevada de Santa Marta and adjacent regions, Colombian Caribbean: Tectonic setting and implications within Pangea paleogeography. *Journal of South American Earth Sciences*, 29(4), 772–783. <https://doi.org/10.1016/j.jsames.2009.12.005>
- Castellanos-Alarcón, O. M., Ríos-Reyes, C. A., & García-Ramírez, C. A. (2016). Occurrence of chloritoid-bearing metapelitic rocks and their significance in the metamorphism of the Silgará Formation at the Central Santander Massif. *Boletín de Ciencias de La Tierra*, 40, 5–15. <https://doi.org/10.15446/rbct.n40.48416>
- Colletta, B., Roure, F., de Toni, B., Loureiro, D., Passalacqua, H., & Gou, Y. (1997). Tectonic inheritance, crustal architecture, and contrasting structural styles in the Venezuela Andes. *Tectonics*, 16(5), 777–794.

- Colmenares, F., Mesa, A., Roncancio, J., Arciniegas, E., Pedraza, P., Cardona, A., Romero, A., Silva, C., Alvarado, S., Romero, O., & Vargas, A. (2007). *Geología De La Planchas 11, 12, 13, 14, 18, 19, 20, 21, 25, 26, 27, 33 Y 34*. Proyecto: "Evolución Geohistórica de La Sierra Nevada de Santa Marta". Ministerio de Minas y Energía, Instituto Colombiano de Geología y Minería e Ingeominas. <http://recordcenter.sgc.gov.co/B12/23008010018162/documento/pdf/2105181621101000.pdf>
- Cordani, U. G., Cardona, A., Jimenez, D. M., Liu, D., & Nutman, A. P. (2005). Geochronology of Proterozoic basement inliers in the Colombian Andes: Tectonic history of remnants of a fragmented Grenville belt. *Geological Society, London, Special Publications*, 246(1), 329–346.
- Cornell, R. M., & Schwertmann, U. (2003). *The Iron Oxides: Structure, Properties, Reactions, Occurrences and Uses* (2003 John Wiley & Sons (ed.)). Wiley. https://books.google.com.co/books?id=dIMuE3_kIW4C
- Dare, S., Barnes, S.-J., & Beaudoin, G. (2015). Did the massive magnetite "lava flows" of El Laco (Chile) form by magmatic or hydrothermal processes? New constraints from magnetite composition by LA-ICP-MS. *Mineralium Deposita*, 50(5), 607–617. <https://doi.org/10.1007/s00126-014-0560-1>
- Doolan, B. (1970). Structure and metamorphism of the Santa Marta Area Colombia. *South America [Microform]*: https://www.researchgate.net/publication/34351494_Structure_and_metamorphism_of_the_Santa_Marta_Area_Colombia_South_America_microform (Accessed 20 July 2016), 200.
- Doolan, B. L., & MacDonald, W. D. (1970). The structure and metamorphism of the Santa Marta Area. *PhD Tesis, State Univ. New York at Binghamton*.
- Formoso, M. L. L. (2006). Some topics on geochemistry of weathering: a review. *Anais Da Academia Brasileira de Ciências*, 78, 809–820.
- García-González, M., Cruz-Guevara, L., Mier-Umaña, R., Vásquez-Pinto, M., Jiménez-Jácome, M., & Moreno-Castellanos, M. (2009). *Evolución térmica de la Subcuenca de la Baja Guajira*. Contrato N° 56 de 2008 UIS-ANH.
- Herrera, P., Escobar, M., Ordoñez, O., & Pimentel, M. (2008). Consideraciones petrográficas, geoquímicas y geocronológicas de la parte occidental del Batolito de Santa Marta. *Dyna*, 75(155), 223–236.
- Irving, E. M. (1975). *Structural evolution of the northernmost Andes, Colombia*.

- Kellogg, J. N. (1984). Cenozoic tectonic history of the Sierra de Perijá, Venezuela-Colombia, and adjacent basins. In W. E. Bonini, R. B. Hargraves, & R. Shagam (Eds.), *The Caribbean-South American Plate Boundary and Regional Tectonics* (Vol. 162, p. 0). Geological Society of America. <https://doi.org/10.1130/MEM162-p239>
- Lizcano-Cabeza, J. A., Ávila-Ascanio, L. F., Ríos-Reyes, C. A., & Vargas-Fiallo, L. Y. (2015a). A comparative study of two aging and fusion methods in the synthesis of zeolitic materials from natural clinker. *DYNA (Colombia)*, 82(193), 32–38. <https://doi.org/10.15446/dyna.v82n193.44217>
- Lizcano-Cabeza, J. A., Ávila-Ascanio, L. F., Ríos-Reyes, C. A., & Vargas-Fiallo, L. Y. (2015b). Efecto del proceso de fusión y envejecimiento en la síntesis de zeotipos a partir de cenizas volantes. *Revista Facultad de Ingeniería*, 1(74), 213–225.
- MacDONALD, W., Doolan, B., & Cordani, U. (1971). Cretaceous-Early Tertiary Metamorphic K-Ar Age Values from the South Caribbean. *GSA Bulletin*, 82(5), 1381–1388. [https://doi.org/10.1130/0016-7606\(1971\)82\[1381:CTMKAV\]2.0.CO;2](https://doi.org/10.1130/0016-7606(1971)82[1381:CTMKAV]2.0.CO;2)
- Molina, A. C., Cordani, U. G., & MacDonald, W. D. (2006). Tectonic correlations of pre-Mesozoic crust from the northern termination of the Colombian Andes, Caribbean region. *Journal of South American Earth Sciences*, 21(4), 337–354.
- Montes, C., Guzman, G., Bayona, G., Cardona, A., Valencia, V., & Jaramillo, C. (2010). Clockwise rotation of the Santa Marta massif and simultaneous Paleogene to Neogene deformation of the Plato-San Jorge and Cesar-Ranchería basins. *Journal of South American Earth Sciences*, 29(4), 832–848.
- Montes, C., Hatcher Jr, R. D., & Restrepo-Pace, P. A. (2005). Tectonic reconstruction of the northern Andean blocks: Oblique convergence and rotations derived from the kinematics of the Piedras–Girardot area, Colombia. *Tectonophysics*, 399(1–4), 221–250.
- Ordóñez, O., Pimentel, M., & de Moraes, R. (2002). Granulitas de los mangos, un fragmento grenvilliano en la parte oriental de la Sierra Nevada de Santa Marta. *Revista de la Academia Colombiana de Ciencias Exactas, Físicas y Naturales*, 26(99), 169–179.
- Paciornik, S., & Gomes, O. D. M. (2009). Co-site Microscopy: Case Studies. *Practical Metallography*, 46(9), 483–498. <https://doi.org/doi:10.3139/147.110047>
- Radelli, L. (1962). Introducción al estudio de la geología y de la petrografía del Macizo de Santa Marta (Magdalena-Colombia). *Geología Colombiana*, 2(0 SE-Artículos), 41–115. <https://revistas.unal.edu.co/index.php/geocol/article/view/30349>
- Rathinasamy, A., & Saliha, B. (2017). *Fundamentals of Soil Science*. Scientific publishers.

- Restrepo-Pace, P., Ruiz, J., Gehrels, G., & Cosca, M. (1997). Geochronology and Nd isotopic data of Grenville-age rocks in the Colombian Andes: new constraints for Late Proterozoic-Early Paleozoic paleocontinental reconstructions of the Americas. *Earth and Planetary Science Letters*, 150(3), 427–441. [https://doi.org/10.1016/S0012-821X\(97\)00091-5](https://doi.org/10.1016/S0012-821X(97)00091-5)
- Ríos, C., Castellanos, O., Ríos R., C., & Castellanos Alarcón, O. (2014). First report and significance of the staurolite metabasites associated to a sequence of calc-silicate rocks from the Silgará Formation at the central Santander Massif, Colombia. *Revista de La Academia Colombiana de Ciencias Exactas, Físicas y Naturales*, 38(149), 418–429.
- Sharma, B. K. (2014). *Environmental chemistry*. Krishna Prakashan Media.
- Stanton, R. L., & Stanton, R. L. (1972). *Ore petrology*. McGraw-Hill Companies.
- Tschanz, C. M., Jimeno, A., & Vesga, C. (1969). Geology of the Sierra Nevada de Santa Marta area (Colombia). *Instituto de Investigaciones e Información Geocientífica, Minero-Ambiental y Nuclear, República de Colombia*, 288.
- Tschanz, C., Marvin, R., Cruz B., J., Mehnert, H., & Cebula, G. (1974). Geologic Evolution of the Sierra Nevada de Santa Marta, Northeastern Colombia. *GSA Bulletin*, 85(2), 273–284. [https://doi.org/10.1130/0016-7606\(1974\)85<273:GEOTSN>2.0.CO;2](https://doi.org/10.1130/0016-7606(1974)85<273:GEOTSN>2.0.CO;2)
- Ussher, S. J., Achterberg, E. P., & Worsfold, P. J. (2004). Marine Biogeochemistry of Iron. *Environmental Chemistry*, 1(2), 67–80. <https://doi.org/10.1071/EN04053>

